

## REPORT DOCUMENTATION PAGE

AFRL-SR-AR-TR-03-

Public reporting burden for this collection of information is estimated to average 1 hour per response, including the time for reviewing instructions, searching existing data sources, gathering and maintaining the data needed, and completing and reviewing this collection of information. Send comments regarding this burden estimate or any other aspect of this collection of information, including suggestions for reducing the burden, to Washington Headquarters Services, Directorate for Information Operations and Reports, 1215 Jefferson Davis Highway, Suite 1204, Arlington, VA 22202-4302, and to the Office of Management and Budget, Paperwork Project, Paperwork Reduction Project (0704-0182).

0282

Aviation

## 1. AGENCY USE ONLY (Leave blank)

## 2. REPORT DATE

## 3. REPORT TYPE AND DATES COVERED

15 NOV 94 TO 14 MAY 99 FINAL

## 4. TITLE AND SUBTITLE

Electromigration and Local Field Effects in Mesoscopic Interconnects

## 5. FUNDING NUMBERS

61102F

2305/ES

## 6. AUTHOR(S)

Professor Bernstein

## 7. PERFORMING ORGANIZATION NAME(S) AND ADDRESS(ES)

UNIVERSITY OF NOTRE DAME  
312 MAIN BUILDING  
NOTRE DAME IN 46556

8. PERFORMING ORGANIZATION  
REPORT NUMBER

## 9. SPONSORING/MONITORING AGENCY NAME(S) AND ADDRESS(ES)

AFOSR/NE  
4015 WILSON BLVD  
SUITE 713  
ARLINGTON VA 22203

10. SPONSORING/MONITORING  
AGENCY REPORT NUMBER

F49620-95-1-0063

## 11. SUPPLEMENTARY NOTES

20030326 015

## 12a. DISTRIBUTION AVAILABILITY STATEMENT

APPROVED FOR PUBLIC RELEASE, DISTRIBUTION UNLIMITED

## 12b. DISTRIBUTION CODE

## 13. ABSTRACT (Maximum 200 words)

Samples were fabricated by the same processes as the previous ones, but with triangular e-beam pads. Validity of the test structure was first examined. After stressing groups of 40 nm and 50 nm wide lines, samples were checked in the FESEM. In the tested samples, most of the lines failed inside the lines and their pads were intact, and a small portion failed in the pads, as shown in Figure 10. The test results show that the new structure can withstand the high current density and survive the bamboo test times. It is normal that a certain percentage of the failures took place in the pads section.

Upon examination of the failure sites, it was found that the sites were always damaged, probably by arcing, similar to that shown in Figure 4. Voids were never found within the lines. There is a possible explanation for the damage where voids are expected. In the wide lines, where voids commonly form due to EM damage, at the final stage of EM, current is concentrated into a very small cross-sectional area, catastrophic damage occurs and the relatively large volume of metal at both sides of the void can be a good heat sink and conduct the heat away in time, leaving a voided open circuit failure. But in the very narrow lines, current density is very high, while the line does not have good dissipation of the heat generated at the final catastrophic stage, resulting in arcing damage at the moment of the open circuit occurs. At present, we don't have direct evidence of what actually happens at the failure sites. Direct insitu observation will help to get more information about it.

## 14. SUBJECT TERMS

## 15. NUMBER OF PAGES

## 16. PRICE CODE

17. SECURITY CLASSIFICATION  
OF REPORT

UNCLASSIFIED

18. SECURITY CLASSIFICATION  
OF THIS PAGE

UNCLASSIFIED

19. SECURITY CLASSIFICATION  
OF ABSTRACT

UNCLASSIFIED

## 20. LIMITATION OF ABSTRACT

UL

Standard Form 298 (Rev. 2-89) (EG)  
Prescribed by ANSI Std. Z39.18  
Designed using Perform Pro, WHS/DIOR, Oct 94

# Final Report

15 Nov 94 - 14 May 99

## 2. Objectives

The objectives of the research have not changed.

## 3. Status of Effort

We continue to investigate the effects of stressing on ultranarrow metal interconnects, with linewidths as narrow as 40 nm. Interesting new phenomena of relatively large, smooth hillocks forming on very narrow lines are being investigated. We have developed a novel technique for utilizing electromigration to create vertically extruded microstructures of controlled cross-sectional shape, discussed in last year's report. AFOSR submitted a patent application entitled, "Planar-Processing Compatible Metallic Micro-Extrusion Process" in September, 1997, which is still pending at the end of the term of this report.

## 4. Accomplishments/New Findings

### 1 Electromigration testing of sub-tenth-micron lines

#### 1.1 EM testing of 60 nm and 90 nm lines

##### A. Sample preparation

Test interconnect lines were fabricated with an SEM-based electron beam lithography (EBL) system developed in our laboratory onto Si substrates with 600 nm thermally grown SiO<sub>2</sub>. Groups of AlCu lines having linewidths of 60 nm, 90 nm and lengths of 60  $\mu$ m with 2  $\mu$ m wide e-beam pads were patterned, followed by electron-beam evaporation of 80 nm thick Al-Cu alloy films from an Al-4.5%Cu evaporation source. It is estimated that this evaporation produced Al-Cu interconnects having approximately between 0.3 and 0.7 at. % Cu. This in-film percentage of Cu is similar to the commonly used Al-0.5% Cu alloy interconnect material. A second-level metallization consisting of a 10 nm Ti adhesion layer followed by 500 nm of Al/Cu was deposited by optical lithography, evaporation and lift off, and was used for bonding pads. The test structure is shown schematically in Figure 1. Samples were annealed at 410°C in forming gas for 30 minutes.

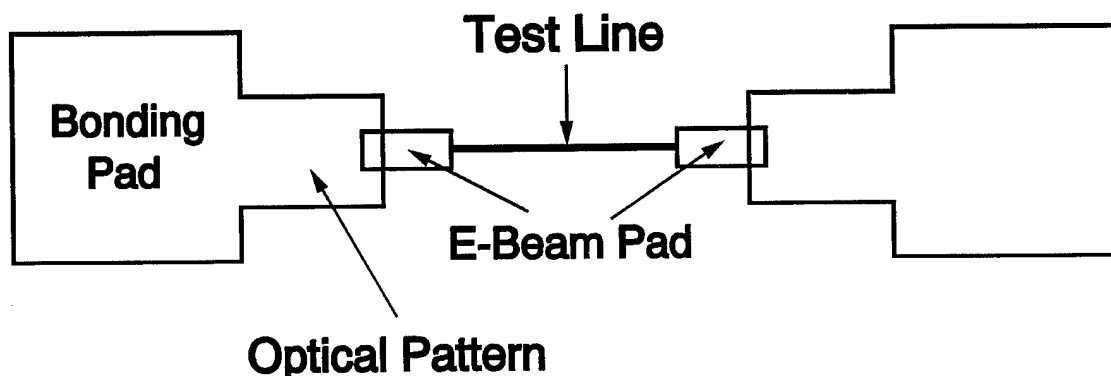


Figure 1. Test structure.

### B. Grain structures

Samples were examined in a Hitachi S-4500 cold-cathode field emission scanning electron microscope (FESEM) before stressing to determine the actual linewidths and the grain sizes in the lines and e-beam pads. Grains in the e-beam pads ranged from 30 nm to 150 nm, and are expected to be the same in the lines, so we conclude that the lines of 60 nm and 90 nm wide were near-bamboo structured, and the lines of 600 nm and 900 nm wide were multi-grain structured. Figure 2 shows the grains in the e-beam pads and in a line of 60 nm width. Grains in the test lines could not be recognized clearly due to the small dimensions and native oxide coating. Figure 3 shows a segment of a line under the normal resolution of the FESEM.

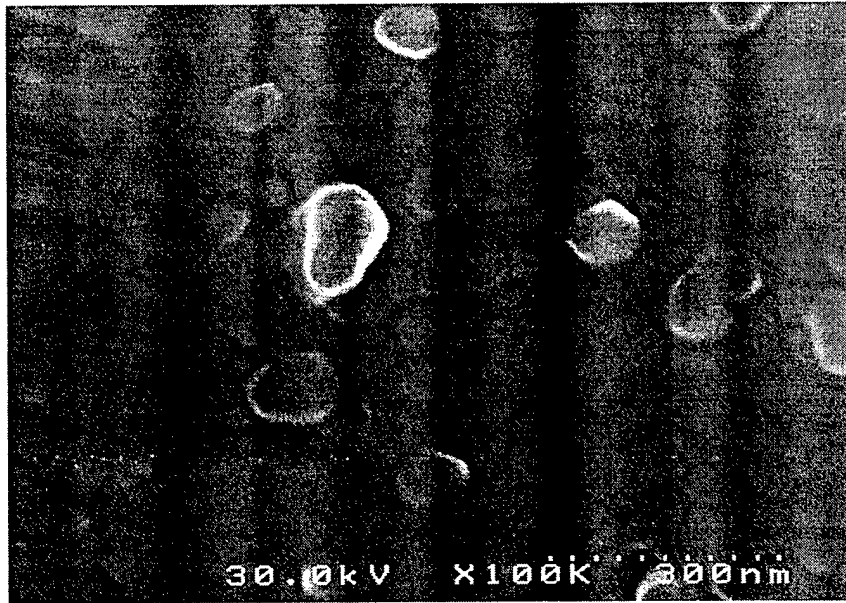


Figure 2. Grains in the e-beam pads.

### C. EM testing

Test samples were mounted in 40-pin ceramic dual in-line packages (DIP) and secured onto a hot stage for heat stressing at 250°C. The hot stage was mounted in an environmental chamber

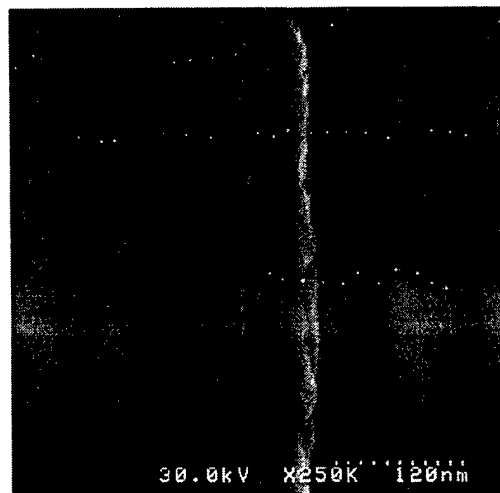


Figure 3. A segment of test line.

that was back-filled with nitrogen gas. Preliminary test results indicated that sub-tenth-micrometer lines had very long lifetimes, on the order of thousands of hours, at a stress current density of  $1 \times 10^6$  A/cm<sup>2</sup>, so the stress current density was set to  $5 \times 10^6$  A/cm<sup>2</sup> in order to observe failures in a feasible time span. Samples were stressed with a constant voltage technique, similar to that reported by Thompson and Cho. The test lines were connected in parallel and a constant voltage, which was found to produce the desired current levels in the lines, was applied.

#### D. Morphology

Examination of the postmortem samples by FESEM revealed several unique EM features for these sub-tenth-micrometer lines, different from what is usually observed in wider unpassivated test lines. First, only a small portion of the lines failed inside the lines themselves, as shown in Figure 4, and most of the failures that we could detect were due to loss of material at the joint area between the lines and their upwind e-beam pads, within the e-beam pads of the sub-tenth-micrometer lines, indicating the actual lifetimes for these lines should be longer than the test results, which is already two orders longer than that of control samples. Figure 5 shows a typical failure at the joint. No early failure sites within the lines could be found, even with the FESEM at magnifications approaching 500 kX. We believe that our inability to detect the early failures in the lines with no pad degradation was due to the existence of the native oxide overlayer, and the extremely small amount of material required to be removed to create an open circuit between grain boundaries. In some cases, a large amount of material was transported away from the upwind pads before failure took place, yet we did not find any hillocks in the downwind pads, and the bumps in some of the lines are not big enough to accommodate so much material. In two test structures, open circuit failure took place even inside the e-beam pads.

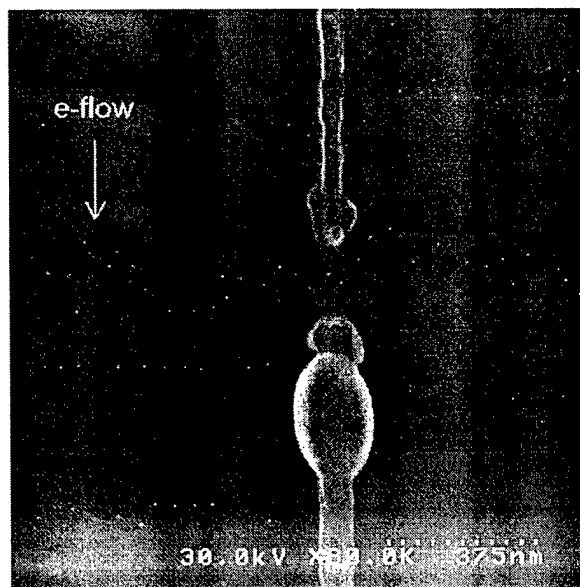


Figure 4. Failure within a 60 nm line. It is believed the front was damaged by an electric arc at the final stage. A narrowed segment and bump also can be clearly seen.

In some lines, bumps of various shapes, primarily spindle or spherical, developed in random segments in the lines. Some lines do not have bumps at all, some have single, or multiple, or two next to each other, as shown in Figure 6.

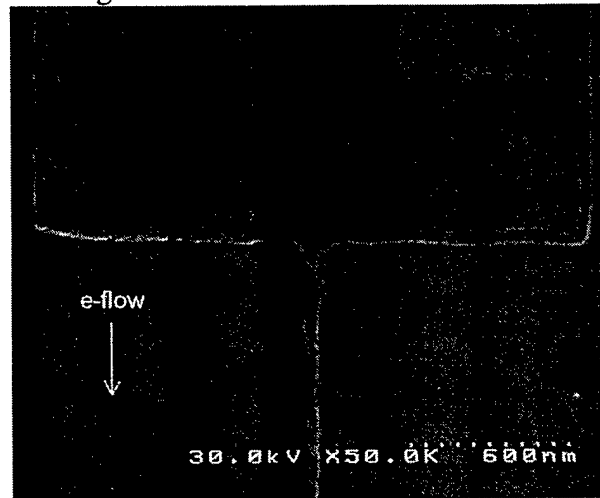


Figure 5. Failure at the joint of a 60 nm line and its e-beam pad.

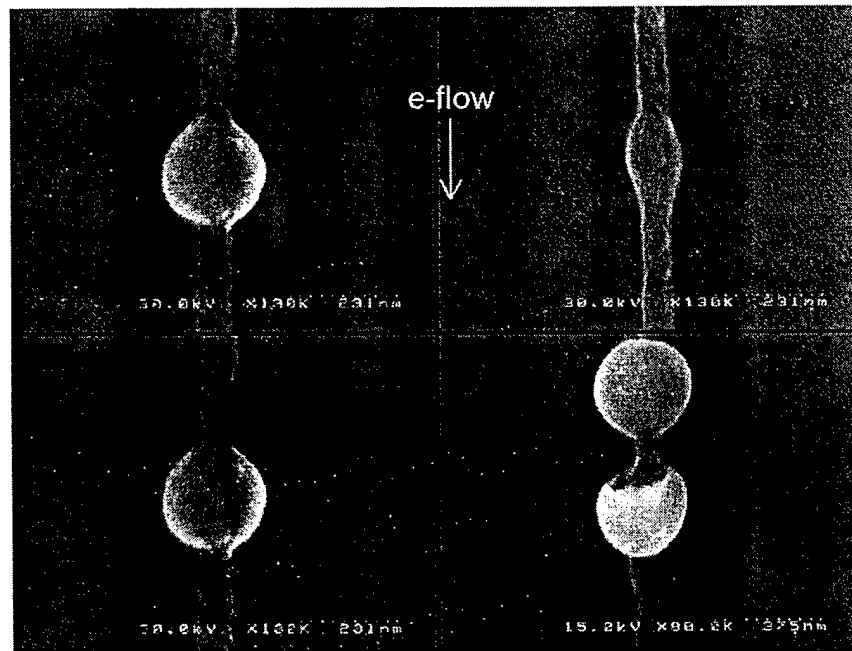
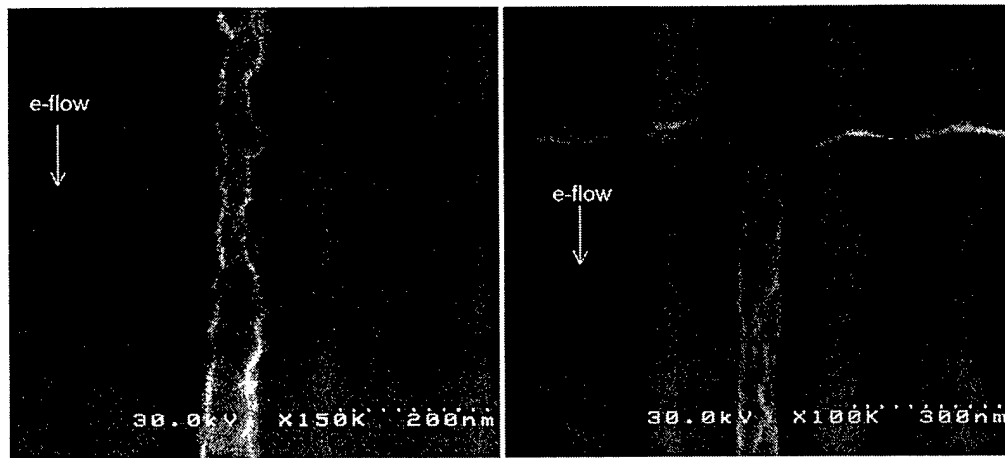


Figure 6. Various shapes of the bumps found in the tested lines.

Another interesting point is that some lines exhibited microstructural changes. Some segments became narrower and bamboo grain structures developed during stress. Figure 7(a) and 7(b) show the narrowed segments and bamboo grain structures. Some segments narrowed down to less than 30 nm. Since it took some time for the structures to develop, we believe the early failures were not within these lines, so the lifetimes of these narrowed lines were at least at the order of hundreds of hours under the aforementioned stress conditions, which were remarkably high.

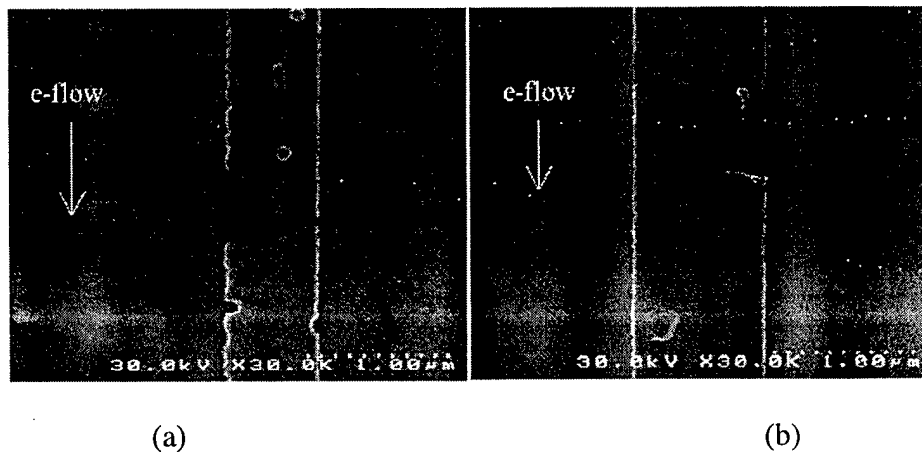


(a) (b)  
Figure 7 Local narrowing in (a) 60 nm and (b) 90 nm lines

We made the e-beam pads more than 20 times wider than the test lines, yet the pads still failed. What we did not expect is that a few failures occurred within the pads, and not at the joint, even in the pads connected to 60 nm lines. These pads were 2  $\mu\text{m}$  wide, which means that some 60 nm wide lines carried the stress current with a density more than 30 times higher than that of the multi-grain pads, and more than 20 times higher in the 90 nm lines. The very high EM resistance may be another indication that a mechanism different from classical EM failure might be working in the sub-tenth-micrometer lines.

#### E. EM in the control samples

Control samples of 600 nm and 900 nm width were fabricated and stressed under the same conditions as for the sub-tenth-micrometer lines. The lifetime measurement data of 600 nm and 900 nm wide fit the lognormal distribution very well. Their lifetimes were in the range of 10 hours, i.e. more than two orders of magnitude shorter than that for the narrow samples, whose lifetimes could be still higher should their e-beam pads have not failed prior to the lines. We also observed voids in upwind lines and hillocks in downwind lines and e-beam pads, as shown in Figure 8, which were common in the literature.



(a) (b)  
Figure 8. Failure sites in control samples of 600 nm and 900 nm width. Void and hillock developments are common in the literature.

## 1.2 EM in 40 nm and 50 nm lines with triangular pads

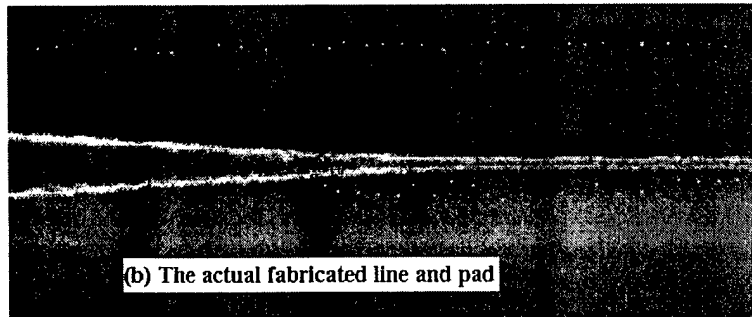
### A. New pattern design

Thermal analysis shows that temperature increase in test lines due to Joule heating at steady-state is proportional to the square of current density. In our previous work, test lines were narrower than 100 nm and lead pads were in the micron range. The huge difference in Joule heating between the lines and the pads can generate a large temperature gradient at the joint of rectangular pads and lines. In the testing of bamboo lines, current density much higher than that for multigrain lines must be applied, making Joule heating an even more serious problem.

Triangular pads with large length-to-width ratio may be a possible way to deal with deep bamboo lines. The narrow part of the triangle connects to the bamboo line, with a gradual increase in linewidth leading to larger patterns, while keeping bamboo structure into the pads as far as possible. Bamboo structure in the pad eventually evolves into multigrain structure. It is reasonable to assume that bamboo lines have similar EM resistance, and wider parts in the pad where current density is lower should have longer MTF than that of the lines of interest. Hopefully the point where the transition occurs, i.e. where the first triple point appears, is far away from the test line and the width at this point is wide enough to compensate the weakness brought by the microstructure change from bamboo into multigrain. In this structure, since there is a gradual change in the linewidth, the temperature gradient effect will also be alleviated. The current crowding effect can also be avoided. A gradual transition between the line and pad will help reduce the problem of current crowding and temperature gradients, especially in the case of Al or Cu, which has a very high thermal conductivity. These considerations lead to the design of small angle triangular pads. In one design, the length of the pad is 20  $\mu\text{m}$  and the end width is 2  $\mu\text{m}$ , as shown in Figure 9(a). After processing, the pattern turned out a smooth transition between the



(a) Triangular pattern and expected bamboo structure



(b) The actual fabricated line and pad

Figure 9. (a) Triangular pad design and (b) the fabricated pattern.

line and the pad, as shown in Figure 9(b). The natural transition due to the continuous exposure during e-beam lithography is actually better than the original design with a change in angle.

## B. Results

Samples were fabricated by the same processes as the previous ones, but with triangular e-beam pads. Validity of the test structure was first examined. After stressing groups of 40 nm and 50 nm wide lines, samples were checked in the FESEM. In the tested samples, most of the lines failed inside the lines and their pads were intact, and a small portion failed in the pads, as shown in Figure 10. The test results show that the new structure can withstand the high current density and survive the bamboo test lines. It is normal that a certain percentage of the failures took place in the pads section.

Upon examination of the failure sites, it was found that the sites were always damaged, probably by arcing, similar to that shown in Figure 4. Voids were never found within the lines. There is a possible explanation for the damage where voids are expected. In the wide lines, where voids commonly form due to EM damage, at the final stage of EM, current is concentrated into a very small cross-sectional area, catastrophic damage occurs and the relatively large volume of metal at both sides of the void can be a good heat sink and conduct the heat away in time, leaving a voided open circuit failure. But in the very narrow lines, current density is very high, while the line does not have good dissipation of the heat generated at the final catastrophic stage, resulting in arcing damage at the moment of the open circuit occurs. At present, we don't have direct evidence of what actually happens at the failure sites. Direct *insitu* observation will help to get more information about it. This is part of the future work. Hillocks also grew in the lines, mostly in the form of spheres and spindles, some of which are larger than the linewidth, and



Figure 10 EM Failure in one of the triangular pads

some have irregular shapes. Figure 11 shows some typical ones. The mechanisms for the formation and growth of these bump-shaped hillocks are as yet unclear. In an *insitu* experiment, bumps were observed to grow very fast only over a short period, and then grow very slowly or stop growing at all, and they were not the cause of line failures. Bump growth happened at all



stages of stressing, not being restricted to any certain period. One series of the hillock growth is shown in Figure 12. It is obvious that an unstable situation developed in some segment of the test line and induced the bump formation and growth. With the growth of the bump, the instability factor gradually disappeared and growth stopped. An interesting aspect to notice is that, after the bumps stop growing, while we believe EM is still underway, the mass flow through the bump is at a balance. Intuitively, at big bumps, current density is lower than both sides of the lines, and mass flow divergence should occur which leads to material accumulation at the upwind side of the bump and material depletion at the downwind side. So once a bump starts to grow, one would expect this unbalanced process to develop, but in reality, this did not happen. More work will be done on it, including *insitu* studies, in order to better understand the underlying mechanisms.

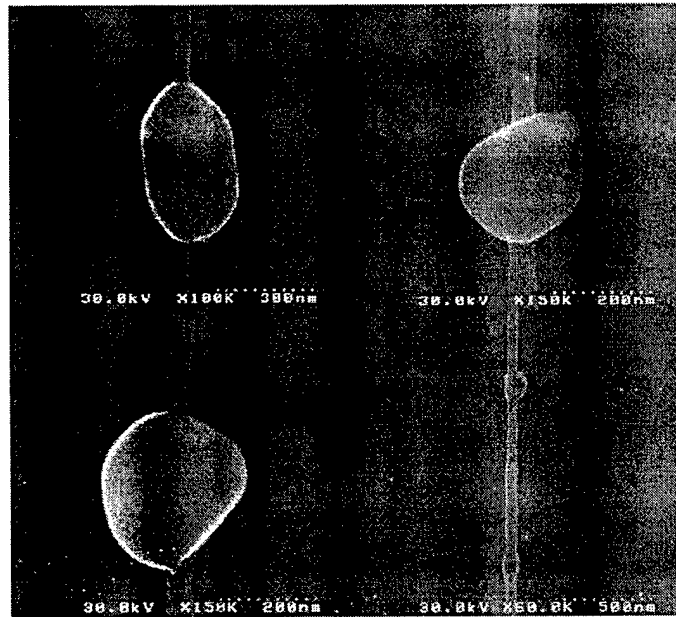


Figure 11 Some irregular-shaped bumps in 40 nm and 50 nm lines

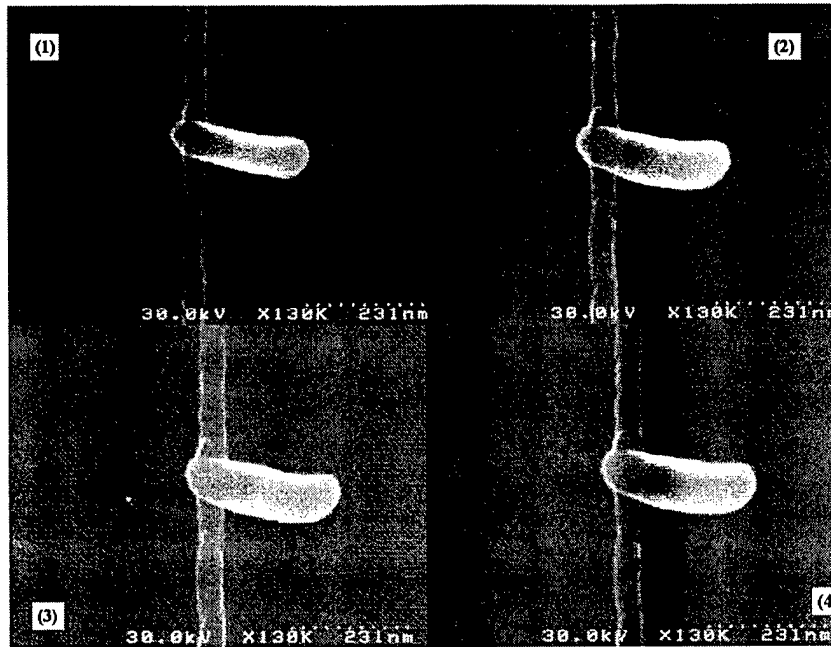


Figure 12 *In situ* observation of bump growth:  
 (1) After 22 hr; (2) After 35 hr; (3) After 54 hr; (4) After 59 hr

## 2. Future Work

### 2.1 Study of EM in AlCu and pure Al lines

Future work on narrow lines will be in the following two areas. First, we will fabricate patterns with triangular pads which make it possible to stress the narrow bamboo lines with large grain size/linewidth ratio and determine the TTF of these lines, including the time span and the distribution mode. Second, perform an *insitu* study of the formation of the bumps and other local structural changes to obtain a better understanding of the dynamics. Serpentine patterns will be used in the *insitu* study to ensure the complete information of the ongoing changes. Attention will also be paid to the final stages, when catastrophic failure occurs.

Narrow lines using pure Al will be fabricated and tested under the same conditions as those for the AlCu alloy lines. In narrow bamboo lines, the role Cu plays is not quite clear. We will compare the EM properties of Cu doped and undoped Al samples and may be able to find some clue.

### 2.2 Study of EM in Cu lines

Narrow lines using Cu will be fabricated using the same evaporation and liftoff process and will be annealed and tested in high vacuum to avoid corrosion in the oxygen ambient. The same or higher current density will be applied to stress the lines. We will be able to access the EM properties of very narrow Cu lines of width in the sub-tenth-micron range for the first time.

### 2.3 *In situ* study

*In situ* observations of EM in interconnect lines are necessary to obtain time-dependent information in order to test current damage formation models as well as to investigate new phenomena. Among the phenomena to be observed will be the microstructure evolution of the lines during stressing, including grain size changes, bump formation and growth, and the manner in which final failures occur. Detailed and systematic studies will be carried out to obtain a better understanding of the different EM behaviors in the narrow super-bamboo lines.

## **5. Personnel Supported**

Professor Gary H. Bernstein and graduate student Pang Xun.

## **6. Publications**

G. H. Bernstein and A. M. Krizan, "Electromigration," to appear in the *Encyclopedia of Electrical and Electronics Engineering*, John Webster, Ed., John-Wiley and Sons, Inc., New York.

The following publication was submitted in the previous year, but appeared in print during the year reviewed in this report.

R. Frankovic and G. H. Bernstein, "In-Situ Observations of Electromigration-Induced Void Dynamics," in *In-Situ Electron and Tunneling Microscopy of Dynamic Processes*, ed. by R. Sharma, M. G-Josifovska, P.L. Gai, R. Sinclair, and L.J. Whitman, MRS Pittsburgh Symposium Proceedings, **404**, pp. 163-169 (1996).

## **7. Interactions/Transitions**

### **a. Participation/presentations at meetings, conferences, seminars, etc.**

X. Pang and G. H. Bernstein, "Electromigration in Ultranarrow Interconnects," presented at the *Fine Line Task Force Meeting*, Blue Mountain Lake, NY, September 1997.

### **b. Consultative and advisory functions...**

none

### **c. Transitions**

## **8. New Discoveries...**

none

## **9. Honors/Awards**

Gary H. Bernstein promoted to Full Professor.